Shape Memory Alloys: Micromechanical Modeling and Numerical Analysis of Structures

V. I. LEVITAS*

Texas Tech University, Department of Mechanical Engineering, Lubbock, TX 79409-1021

A. V. IDESMAN AND E. STEIN

University of Hannover, Institute of Structural & Computational Mechanics, Appelstraße 9A, 30167 Hannover, Germany

ABSTRACT: Multiscale modeling of structures made from shape memory alloys (SMA) is presented. Starting with consideration of a single transformation event at the micro-level and averaging over the representative volume, micromechanically-based macroscopic constitutive equations are derived, which are used in Finite Element Method (FEM) code to model the behaviour of structures. Using the thermodynamic theory of phase transformations (PT) in elastic materials on the micro-level, the macroscopic associated transformation flow rule, the corresponding extremum principle and the nonconcavity of the transformation surface are derived for transformational micromechanisms of inelastic deformation due to phase transformation, twinning and reorientation of martensitic variants. A simple three-dimensional micromechanically-based model for thermoelastic martensitic PT is presented. The model is transformed to the fashion similar to that for J_2-plasticity theory. It allows one to modify the FEM for elastoplasticity (including the radial return algorithm for numerical integration of the constitutive equations and calculation of the consistent tangent moduli) in order to model PT in SMA. Some axisymmetric problems for PT in SMA tubes are solved. In particular, PT regularities of a tube assembly with a SMA cylinder element are investigated at different external conditions.

INTRODUCTION

ADEQUATE mathematical models and consistent numerical methods play a very important role in the design and development of control methods for structures made from smart materials. A key point in mathematical simulation is the derivation of reliable and simple three-dimensional constitutive equations describing the deformation of SMA. Another is the development of effective and robust numerical methods. The mechanisms of inelastic behavior of SMA are related to martensitic PT of the parent phase (austenite) into the product phase (martensite), reverse PT of martensite into austenite and transformation of one martensitic variant into another (reorientation). Deformation twinning and detwinning can be considered as a particular case of PT without a jump in the thermal (chemical) part of the free energy. These processes are connected to the jump-like deformation of crystal lattices which can be described by variation of the transformation strain tensor $\bar{\varepsilon}^t$ from its initial value $\bar{\varepsilon}_1^t$ to final value $\bar{\varepsilon}_2^t$. The transformation strain for twinning is simple shear. For classical micromechanisms of the plastic deformation of metals, like dislocation motion or macroscopic shearing along slip directions in single crystals, it is possible to prove the validity of the macroscopic associated flow rule [Hill (1967), Rice (1971)]. It is shown using either the

micromechanical approach [Hill (1967), Mandel (1966)] or the method of internal variables [Rice (1971), Nemat-Nasser (1975)] that if the associated flow rule is valid at the micro-level (for each point of representative volume) then it is valid at the macro-level (for the entire representative volume).

Such research has not been completed for SMA. There are several papers in which some general relations for representative volume of elastoplastic material with moving interfaces are considered [Leblond et al. (1989), Levitas (1992, 1996), Pradeilles-Duval and Stolz (1993)]. However, no result related to the macroscopic normality rule was obtained. Moreover, PT is related not only to a moving interface, but to the nucleation process as well. To the authors' best knowledge, the only papers combining micro- to macro-transition with consideration of the nucleation process are by Levitas and Stein (1997) and Levitas, Idesman, Stein et al. (1999), however under some special constraints on admissible stress and strain fields.

The goals of this paper are:

- to develop the method of micro-macro transition for transformational mechanisms of inelastic deformation including both nucleation and interface propagation and to derive some general properties of macroscopic constitutive equations for SMA
- to formulate a micromechanically-based simple three-dimensional model for SMA consistent with the

---

*Author to whom correspondence should be addressed.

general properties derived and to substantiate the similarity between phase transition theory and J_2-plasticity theory
- to present an algorithm for finite element (FE) solution of boundary-value problems using the above similarity
- as an illustration, to solve numerically a set of problems related to tube connection by using the shape memory effect

Having set forth these goals, a quite rational and economic multiscale description of SMA structures was developed.

The following symbolic tensor notations are used throughout this paper: vectors and tensors are denoted in boldface type; $A \cdot B$ and $A:B$ are contractions of tensors over one or two indices; := means equals per definition; the Euclidian norm $|A| := (A:A)^{1/2}$ is the modulus (amplitude) of tensor A; $(A)_s$ represents the symmetric part of tensor A.

MICROMECHANICAL DERIVATION OF THE MACROSCOPIC TRANSFORMATION FLOW RULE

There are two important differences between slip and transformational mechanisms of inelastic deformation which make impossible an application of the methods developed for classical plasticity [(Hill (1967), Mandel (1966), Rice (1971), Nemat-Nasser (1975)].

1. At the micro-level (for each material point of the representative volume) it is possible to describe the slip mechanism by infinitesimal increments of inelastic strain. The change in transformation strain $\tilde{\epsilon}_2^t - \tilde{\epsilon}_1^t$ is always finite. For each PT or twinning the transformation strain $\tilde{\epsilon}_2^t$ represents a set of symmetry-related constant tensors, transformation strain $\tilde{\epsilon}_1^t = 0$. All intermediate values of transformation strains $\tilde{\epsilon}^t$ are unstable and cannot exist in equilibrium.
2. At the micro-level, there is a local constitutive equation for the slip mechanism, but there is no local constitutive equation for transformation strain $\tilde{\epsilon}_2^t$. PT criterion is nonlocal, and to choose the actual $\tilde{\epsilon}_2^t$ in each point of a nucleus among a finite number of crystallographically admissible martensitic variants, as well as a position and shape of nucleus, an extremum principle for the whole nucleus is used [see Levitas (1998), as well as Equations (9) and (16)]. Even if we assume that distribution of transformation strain in the nucleus can be determined by crystallographic theory of martensitic PT proposed by Weschler, Liberman and Read or Bowles and Mackenzie [see e.g., Wayman (1964)], then nonlocal PT criterion and extremum principle are necessary to determine the shape and position of the nucleus and one of invariant plane variant among all crystallographically admissible.

Considered here is the particular case when elastic properties do not change during PT; deformations are small, and the elasticity law is linear. Consider a representative volume V of multiphase material (Figure 1) under macroscopically ho-
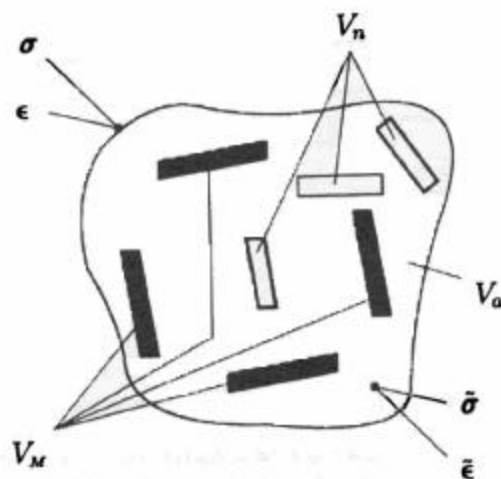

Figure 1. Representative volume V with existing martensite V_m and multi-connected currently transforming region V_n inside austenitic matrix V_a.

mogeneous boundary conditions [Hill (1967), Havner (1971)].

An additive decomposition is adopted for local and for macroscopic strains

$$\tilde{\epsilon} = \tilde{\epsilon}^e + \tilde{\epsilon}^t; \quad \epsilon = \epsilon^e + \epsilon^t \tag{1}$$

where ϵ and ϵ^e are the macroscopic total and elastic strains and ~ denotes local fields. Macroscopic stress and strain are local stress and strain averaged over the volume V, i.e.,

$$\sigma = \frac{1}{V}\int_V \tilde{\sigma}dV = \langle \tilde{\sigma} \rangle \tag{2}$$

$$\epsilon = \frac{1}{V}\int_V \tilde{\epsilon}dV = \langle \tilde{\epsilon} \rangle \tag{3}$$

where $\langle ... \rangle$ means an averaging over the representative volume V.

Let us concentrate on direct martensitic PT and divide the volume V into three parts (Figure 1): the infinitesimal volume V_n in which during time Δt PT occurs and parts of austenite V_a and martensite V_m which do not transform during time Δt. Volume V_n may be a new nucleus or volume covered by an interface Σ moving with velocity v_n during time Δt, i.e., $dV_n = v_n\Delta t d\Sigma$. The following expression for the local stresses is valid for a linear elastic solid:

$$\tilde{\sigma}(r) = \sigma : A(r) + \int_{V_m} G(r,r') : \tilde{\epsilon}^t(r')dr'$$

$$+ \int_{V_n} G(r,r') : \tilde{\epsilon}^t(r')dr' \tag{4}$$

where r is the position vector, A the fourth-rank localization tensor and G the Green function for internal stresses. Equation (4) is the consequence of the linear response to external

stresses σ and inelastic strains. Tensor A can be determined by solution of the linear elastic problem for representative volume without PT. As elastic constants are assumed to be the same before and after PT, tensor A is constant. For homogeneously distributed elastic constants (e.g., a single crystal or isotropic material) tensor A is the fourth-rank identity tensor. For macroscopic transformation strain, the Mandel (1966) formula

$$\epsilon^t = \langle A : \tilde{\epsilon}^t \rangle \tag{5}$$

is valid. Now an equation for the rate of macroscopic transformation strain will be derived. By definition it holds

$$\epsilon^t(t) = \langle A : \tilde{\epsilon}^t(t) \rangle \tag{6}$$

$$\epsilon^t(t+\Delta t) = \langle A : \tilde{\epsilon}^t(t) \rangle + \langle A : (\tilde{\epsilon}_2^t - \tilde{\epsilon}_1^t) \rangle_n \frac{V_n}{V}$$

$$= \epsilon^t(t) + \langle A : (\tilde{\epsilon}_2^t - \tilde{\epsilon}_1^t) \rangle_n \frac{V_n}{V} \tag{7}$$

where $\tilde{\epsilon}_1^t$ and $\tilde{\epsilon}_2^t$ represent the transformation strain before (i.e., at time t) and after (i.e., at time $t + \Delta t$) PT in the transforming volume V_n, and

$$\langle ... \rangle_n = \frac{1}{V_n} \int_{V_n} (...) dV_n$$

is the average over the nucleus V_n. For direct PT, $\tilde{\epsilon}_1^t = 0$ and Equation (7) takes into account the appearance of transformation strain $\tilde{\epsilon}_2^t$ in the volume V_n. Equation (7) is also valid for reverse PT and reorientation of martensitic variants. In this case, nucleus V_n belongs to volume V_m and in addition to the appearance of transformation strain $\tilde{\epsilon}_2^t$ Equation (7) takes into account the fact that transformation strain $\tilde{\epsilon}_1^t$ disappears in the volume V_n. For the reverse PT, $\tilde{\epsilon}_1^t$ is given and $\tilde{\epsilon}_2^t = 0$. Introducing the volume fraction of martensite $c := V_m/V$ and the rate of volume fraction of martensite $\dot{c} := V_n/V\Delta t$ (the change in martensite volume is V_n) at $\Delta t \to 0$ and $V_n \to 0$, we obtain from Equation (7)

$$\dot{\epsilon}^t = \dot{c} \langle A : (\tilde{\epsilon}_2^t - \tilde{\epsilon}_1^t) \rangle_n \quad \text{or} \quad \frac{\partial \epsilon^t}{\partial c} = \langle A : (\tilde{\epsilon}_2^t - \tilde{\epsilon}_1^t) \rangle_n \tag{8}$$

The PT criterion is applied in the following form [Levitas (1998), Levitas and Stein (1997)]

$$\left\langle \int_{\tilde{\epsilon}_1^t}^{\tilde{\epsilon}_2^t} \tilde{\sigma} : d\tilde{\epsilon}^t \right\rangle - \Delta\psi^\theta - k_n = 0 \tag{9}$$

where $\Delta\psi^\theta$ is the change in the thermal part of free energy which is an experimentally determined function of temperature. As temperature variation during the transformation event is not included in this paper, $\Delta\psi^\theta$ is a constant. To cal-

culate the transformation work in Equation (9), one must vary the transformation strain $\tilde{\epsilon}^t$ in the nucleus from $\tilde{\epsilon}_1^t$ to $\tilde{\epsilon}_2^t$ and for each $\tilde{\epsilon}^t$ calculate corresponding stress $\tilde{\sigma}$ by solution of the elastic boundary-value problem. Equation (9) means that the calculated value of the dissipation increment during the complete PT in region V_n reaches its actual (experimentally determined) value k_n.

Macroscopic transformation surface shall now be defined. Macroscopic stresses σ^*, for which corresponding local stresses

$$\tilde{\sigma}^*(r) = \sigma^* : A(r) + \int_{V_m} G(r,r') : \tilde{\epsilon}^t(r') dr'$$

$$+ \int_{V_n} G(r,r') : \tilde{\epsilon}^t(r') dr' \tag{10}$$

satisfy the inequality

$$\left\langle \int_{\tilde{\epsilon}_1^t}^{\tilde{\epsilon}_2^t} \tilde{\sigma}^* : d\tilde{\epsilon}^t \right\rangle - \Delta\psi^\theta - k_n < 0 \tag{11}$$

for all admissible fields $\tilde{\epsilon}_2^t$, $\tilde{\epsilon}_1^t$ and V_n define the region in the macroscopic stress space $\varphi(\sigma^*, \ldots, c + c_n) < 0$, $c_n := V_n/V = \Delta c$ where PT for the given volume fraction increment c_n is impossible (because the PT criterion is not satisfied). At the surface $\varphi(\sigma, \ldots, c + c_n) = 0$, PT condition (9) is satisfied, i.e., PT can occur.

As the main assumption we use the postulate of realizability [Levitas (1995, 1998)]: as soon as PT can occur from the point of view of thermodynamics, it will occur, i.e., the first fulfillment of the necessary energetic condition (9) is sufficient for the occurrence of PT.

Consequently, condition $\varphi(\sigma, \ldots, c + c_n) = 0$ defines the surface in the macroscopic stress space where PT occurs with the given c_n, i.e., the PT surface. As $c_n \to 0$ we obtain PT surface $\varphi(\sigma, \ldots, c) = 0$ which is completely similar to the yield surface for slip mechanisms of plasticity, i.e., it is independent of an infinitesimal increment of some parameters. Condition $\varphi(\sigma, \ldots, c + c_n) = 0$, which is necessary and sufficient for the occurrence of PT in some volume V_n during the time Δt, can be presented in the following form

$$\varphi(\sigma(t+\Delta t), \ldots, c(t+\Delta t)) = 0$$

$$= \varphi(\sigma(t), \ldots, c(t)) + \dot{\varphi}(\sigma(t), \ldots, c(t))\Delta t \tag{12}$$

This equation due to arbitrariness of Δt results in $\varphi(\sigma, \ldots, c) = 0$ and $\dot{\varphi}(\sigma, \ldots, c) = 0$. We arrive at a definition of loading-unloading conditions similar to those in plasticity theory:

$$\text{at } \varphi(\sigma^*, . \quad , c) < 0 \Rightarrow \text{PT does not occur} \tag{13}$$

$$\text{at } \varphi(\sigma, \ldots, c) = 0 \quad \text{and} \quad \dot{\varphi}(\sigma, \ldots, c) = 0 \Rightarrow \text{PT occurs} \tag{14}$$

Equation $(14)_2$ is called the consistency condition in plasticity theory. The combination of Equations (9) and (11) results in the extremum principle

$$\left\langle \int_{\tilde{\varepsilon}_1^t}^{\tilde{\varepsilon}_2^t} \tilde{\sigma} : d\tilde{\varepsilon}^t \right\rangle - \Delta\psi^\theta - k_n = 0 > \left\langle \int_{\tilde{\varepsilon}_1^t}^{\tilde{\varepsilon}_2^t} \tilde{\sigma}^* : d\tilde{\varepsilon}^t \right\rangle_n - \Delta\psi^\theta - k_n$$

at $\varphi(\sigma, \quad , c+c_n) = 0 > \varphi(\sigma^*, \quad , c+c_n)$ (15)

which is equivalent to *the principle of the maximum of averaged microscopic transformation work*

$$\left\langle \int_{\tilde{\varepsilon}_1^t}^{\tilde{\varepsilon}_2^t} \tilde{\sigma} : d\tilde{\varepsilon}^t \right\rangle_n > \left\langle \int_{\tilde{\varepsilon}_1^t}^{\tilde{\varepsilon}_2^t} \tilde{\sigma}^* : d\tilde{\varepsilon}^t \right\rangle_n$$

at $\varphi(\sigma, . \quad , c+c_n) = 0 > \varphi(\sigma^*, \ldots, c+c_n)$ (16)

Let us derive corresponding extremum principle at the macrolevel. In volume V_m, transformation strains do not change during time Δt, and in volume V_n, they vary from $\tilde{\varepsilon}_1^t$ to $\tilde{\varepsilon}_2^t$. The extremum principle (16) allows one to determine the shape and position of the nucleus V_n as well as the distribution of transformation strain $\tilde{\varepsilon}_2^t$ within it.

After substitution of Equation (4) into the left part of Equation (16) and integration we obtain the transformation work per unit volume V_n

$$\frac{1}{V_n} \int_{V_n} \int_{\tilde{\varepsilon}_1^t}^{\tilde{\varepsilon}_2^t} \tilde{\sigma} : d\tilde{\varepsilon}^t dV_n = \sigma : \left\langle A : (\tilde{\varepsilon}_2^t - \tilde{\varepsilon}_1^t) \right\rangle_n$$

$$+ \frac{1}{V_n} \int_{V_n} \int_{V_m} (\tilde{\varepsilon}_2^t(r) - \tilde{\varepsilon}_1^t(r)) : G(r,r') : \tilde{\varepsilon}_2^t(r')drdr'$$

$$+ \frac{1}{2V_n} \int_{V_n} \int_{V_n} (\tilde{\varepsilon}_2^t(r) - \tilde{\varepsilon}_1^t(r)) : G(r,r') : (\tilde{\varepsilon}_2^t(r') - \tilde{\varepsilon}_1^t(r'))drdr'$$

(17)

Using Equation (8) as $V_n \to 0$ we obtain

$$\sigma : \left\langle A : (\tilde{\varepsilon}_2^t - \tilde{\varepsilon}_1^t) \right\rangle_n = \sigma : \frac{1}{\dot{c}} \dot{\varepsilon}^t = \sigma \frac{\partial \varepsilon^t}{\partial c}$$ (18)

Consequently, the first term in Equation (17) is the macroscopic transformation work per unit volume fraction increment and per unit representative volume, the second term represents the interaction energy between transformation strain in a volume V_m and the jump of transformation strain in transforming volume V_n, and the third term is the energy of internal stresses in the transforming volume V_n. For the stresses σ^* in the principle Equation (16) we obtain the same expression with σ^* instead of σ. After substitution of these expressions in principle Equation (16) at $c_n \to 0$ one obtains extremum principle in terms of macroscopic variables only

$$\sigma : \dot{\varepsilon}^t > \sigma^* : \dot{\varepsilon}^t \quad \text{at} \quad \varphi(\sigma, \quad = 0 > \varphi(\sigma^*, \ldots$$ (19)

i.e., the principle of the maximum of macroscopic transformation power. Principle (19) coincides with the known extremum principle in phenomenological plasticity theory. Using it, the associated transformation flow rule

$$\dot{\varepsilon}^t = h\frac{\partial\varphi}{\partial\sigma}$$ (20)

can be derived for a smooth transformation surface and the corresponding expression for a singular point at the transformation surface. Here h is the Lagrange multiplier which is determined with the help of consistency condition Equation (14). The nonconcavity of the PT-surface follows from Equations (19) and (20) as well (Figure 2). Consequently, despite the essential physical and formal difference in comparison to the case of plasticity due to slip mechanisms, the associated flow rule is proved for the transformation mechanisms of inelastic straining as well.

It is possible to prove that $h = \dot{c}$ and the kinetic equation for the rate of volume fraction of martensite can be found from consistency condition Equation (14).

What do all the above results mean in practice? A priori, one needs seven scalar equations: an equation for the PT surface, a kinetic equation for the rate of martensite volume fraction and five equations for the deviatoric transformation strain rate (volumetric transformation strain rate is equal to the product of the local volumetric transformation strain and $\dot{c}$). It is proven above for a quite general case that only one equation is needed for the PT surface, and the remaining six equations can be derived from it.

Similar results can be obtained for the reverse PT (or reorientation process): the rate of macroscopic transformation strain due to reverse PT (reorientation) is orthogonal to the surface of reverse PT (reorientation) in a macroscopic stress space. Surfaces of direct and reverse PT and reorientation can intersect each other, i.e., direct and reverse PT as well as a reorientation process are possible simultaneously in different parts of the representative volume.

Some known experiments under combined torsion and tension [Rogueda et al. (1996), Tanaka et al. (1998)] confirm with reasonable accuracy the validity of the associated transformation rule for direct PT. The reason for the possible devi-
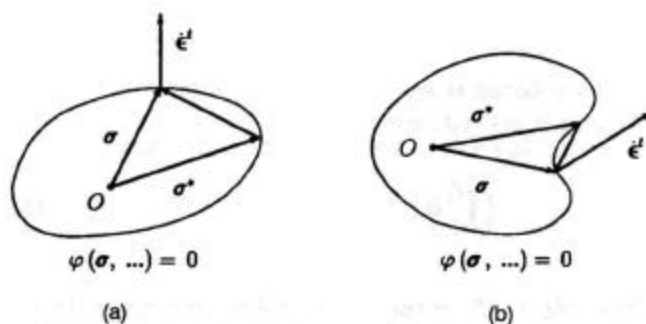

$\varphi(\sigma, \ldots) = 0$ $\varphi(\sigma, \ldots) = 0$

(a)   (b)

Figure 2. (a) Schema of nonconcave PT-surface and associated transformation flow rule; (b) violation of principle Equation (19) for concave PT surface.

ations from Equation (20) in experiments is the same as in slip plasticity, namely the presence of singular points on a transformation surface. Additionally, simultaneous direct and reverse PT and reorientation can occur in different parts of a volume.

A SIMPLE MICROMECHANICAL MODEL FOR PSEUDOELASTIC BEHAVIOR OF CuZnAl ALLOY AND ITS NUMERICAL TREATMENT

The results obtained in the previous section represent a micromechanical basis for the formulation of simplified models for the behavior of SMA. In the first approximation, one can use pure phenomenological models based on prescription of the PT surface $\varphi(\sigma, \ldots, c) = 0$, i.e., as in the phenomenological theory of plasticity. However, it is very difficult to guess or find experimentally this equation. A more advanced approach has to be based on the micromechanical derivation of the equation for a PT surface. A very detailed micromechanical description developed by Patoor, Eberhardt and Berveiller (1996) is very important for describing physics, but it requires time-consuming computations and does not allow the presentation of constitutive equations in analytical form for complex loading processes. An alternative approach is the formulation of a simple noncontradictory analytical three-dimensional micromechanically- and thermodynamically-based model. Such models can be implemented in computer codes for the analysis of structures consisting of intelligent materials. It is clear that these models cannot precisely describe material behavior, and we arrive at the situation similar to the phenomenological plasticity theory. The simplest plastic model with isotropic and kinematic hardening is the most popular for structural analysis and simulation of technological processes, despite the fact that it strongly simplifies reality. An analytical phenomenological thermodynamic SMA model

which is realized in computer code (using an analogy with numerical methods of plasticity) for modeling of structures from SMA is suggested in the paper by Lagoudas et al. (1996). In the paper by Levitas and Stein (1997) a micromechanical model allowing for five micromechanical mechanisms of PT (nucleation at direct austenite → martensite and reverse martensite → austenite PT, interface motion at direct and reverse PT and reorientation of martensitic variants) is proposed. Comparisons with other models, e.g., by Sun and Hwang (1993), are made as well. In this paper we consider a particular case of this model for nucleation for the stress-induced direct austenite → martensite PT only, when the modulus of transformation in nucleus strain reaches its maximum possible value. The detailed derivation of constitutive equations for this case is also presented in the paper by Levitas et al. (1998) with parameter identification using simple tension experiments. This model is not exactly the same as the flow theory of plasticity, because, e.g., the result $h = \dot{c}$ has no counterparts in plasticity theory. However, we succeeded in transforming these equations into the form which is completely similar to that of plasticity theory. The final equations for the model are presented in Table 1 and compared with equations for J_2-plasticity.

Here u is the displacement vector, $I_1(\epsilon^e)$ is the first invariant of ϵ^e; K, G are the elastic bulk and shear moduli, α is the back-stress (using the terminology of plasticity), n is the unit vector in five-dimensional deviatoric stress space (i.e., $|n| = 1$), ϵ^p is the plastic strain tensor, q is the accumulated plastic strain. Function $A(c, \theta)$ is a known material function for PT [see Levitas et al. (1998)],

$$A(c) = \sqrt{\frac{3}{2}}\left[\frac{aP}{2} + \frac{1}{a}(\Delta\psi^\theta(\theta) + k_n(c))\right]$$

$$\Delta\psi^\theta(\theta) = \Delta\psi_0 - \Delta s_0\theta$$

$$k_n(c) = b + dc$$

Table 1. Analogy between the model for SMA and J_2-plasticity.

Phase Transition		Plasticity	
Kinematical decomposition	$\epsilon = (\nabla u)_s = \epsilon^e + \epsilon^t$	Kinematical decomposition	$\epsilon = (\nabla u)_s = \epsilon^e + \epsilon^p$
Hooke's law	$\sigma = KI_1(\epsilon^e)I + 2G \,\text{dev}\, \epsilon^e$	Hooke's law	$\sigma = KI_1(\epsilon^e)I + 2G \,\text{dev}\, \epsilon^e$
PT criterion	$\varphi = |s - \alpha| - \sqrt{\frac{2}{3}}A(c,\theta) = 0$	Yield condition	$\varphi = |s - \alpha| - \sqrt{\frac{2}{3}}f(q,\theta) = 0$
Consistency conditon	$\dot{\varphi} = (s, \alpha, c, \theta) = 0$	Consistency conditon	$\dot{\varphi} = (s, \alpha, q, \theta) = 0$
Associated flow rule	$\dfrac{\dot{\epsilon}^t}{|\dot{\epsilon}^t|} = \dfrac{s - \alpha}{|s - \alpha|} = n$	Associated flow rule	$\dfrac{\dot{\epsilon}^p}{|\dot{\epsilon}^p|} = \dfrac{s - \alpha}{|s - \alpha|} = n$
Evolution equations	$\dot{c} = \dfrac{1}{a}|\dot{\epsilon}^t|$ $\dot{\alpha} = -P\dot{\epsilon}^t$	Evolution equations	$\dot{q} = \sqrt{\dfrac{2}{3}}|\dot{\epsilon}^p|$ $\dot{\alpha} = \dfrac{2}{3}H(q)\dot{\epsilon}^p$
Equilibrium equations	$\nabla \cdot \sigma = 0$	Equilibrium equations	$\nabla \cdot \sigma = 0$

where P characterizes the energy of internal stresses, $a = |\boldsymbol{\epsilon}_{max}^t|$ characterizes the maximum possible transformation strain, e.g., at tension, $\Delta\psi_0$ and Δs_0 are the difference in the reference values of free energy and entropy, $b > 0$ and $d > 0$ are the material parameters. The functions $f(q, \theta)$ and $H(q)$ are defined in plasticity theory [see Simo and Taylor (1985), Simo and Hughes (1998)].

Note that k_n is an increasing function of c. In the space of deviatoric stress, PT criterion represents a sphere with growing radius, and this sphere is shifted on vector $\boldsymbol{\alpha} = -P\boldsymbol{\epsilon}^t$ (Figure 3). The modulus $|\boldsymbol{\epsilon}^t|$ grows when c grows, and at a radial loading the center of the sphere moves in direction opposite to s. Consequently (using similarity with plasticity theory), in space s the material exhibits isotropic hardening and kinematic softening. The transformation strain rate vector $\dot{\boldsymbol{\epsilon}}^t$ is directed along the normal to this sphere. Difference $|s - \boldsymbol{\alpha}|$ has a meaning of mean stress in austenite [Levitas and Stein (1997)].

In order to find the distribution of stresses, strains and volume fraction of martensite for a structure made from SMA using the above described simple model, we have to solve the set of equations presented in the left column of Table 1. Due to the analogy found between the model for SMA and elastoplastic model with kinematic and isotropic hardening [the right column of the Table 1, see Simo and Taylor (1985), Simo and Hughes (1998)], the methods developed for elastoplastic problems may be used. For discretized solutions, the FEM is applied. This solution is realized in a step-by-step form, i.e., with a known solution at time t_n a solution at time t_{n+1} is computed, where n is the step number. When an increment of total strain $\Delta\boldsymbol{\epsilon}$ is known, then the stresses $\boldsymbol{\sigma}$ can be calculated according to the radial return algorithm presented in Box 1 [see Simo and Taylor (1985), Simo and Hughes (1998) for plasticity].

Introducing a new variable $c_1 = a\sqrt{2/3}c$ instead of c we obtain full correspondence between elastoplastic equations and equations for SMA. Then the consistent tangent moduli $c^{n+1} = (\partial\boldsymbol{\sigma}^{n+1})/(\partial\Delta\boldsymbol{\epsilon})$ (which is calculated according to the radial return algorithm) have practically the same form as in the paper by Simo and Taylor (1985) for plasticity, i.e.,
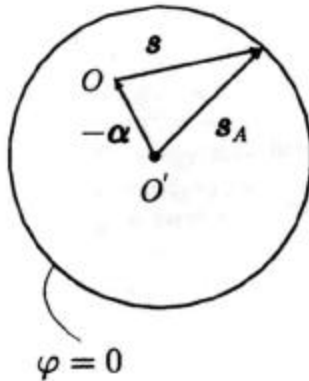

Box 1. The radial return algorithm.

1. Compute trial elastic deviatoric stress s^{trial} (elastic predictor.

$$s^{trial} = s^n + 2G\, dev\, \Delta\boldsymbol{\epsilon} \tag{22}$$

$$\boldsymbol{\xi}^{trial} = s^{trial} + P\boldsymbol{\epsilon}_t^n$$

If $\varphi(s^{trial}, \boldsymbol{\alpha}^n, c^n) = \left|s^{trial} + P\boldsymbol{\epsilon}_t^n\right| - \sqrt{\dfrac{2}{3}}A(c^n) \leq 0$ then $\tag{23}$

$$s^{n+1} = s^{trial} \quad \text{and go to Step 5}$$

2. Compute unit normal field $\bar{n}$

$$\bar{n} = \frac{\boldsymbol{\xi}^{trial}}{\left|\boldsymbol{\xi}^{trial}\right|} \tag{24}$$

3. Compute the increment of the volume fraction of martensite Δc by local iterations from the following nonlinear algebraic equation

$$\left|s^n + 2G(dev\,\Delta\boldsymbol{\epsilon} - a\Delta c\bar{n}) + P(\boldsymbol{\epsilon}_t^n + a\Delta c\bar{n})\right| = \sqrt{\dfrac{2}{3}}A(c^n + \Delta c) \tag{25}$$

4. Compute the volume fraction of martensite c^{n+1}, the transformation strain $\boldsymbol{\epsilon}_t^{n+1}$ and deviatoric stress s^{n+1}

$$c^{n+1} = c^n + \Delta c \tag{26}$$

$$s^{n+1} = s^n + 2G(dev\Delta\boldsymbol{\epsilon} - a\Delta c\bar{n}) \tag{27}$$

$$\boldsymbol{\epsilon}_t^{n+1} = \boldsymbol{\epsilon}_t^n + a\Delta c\bar{n} \tag{28}$$

5. Add the mean stress (due to elastic volume change)

$$\boldsymbol{\sigma}^{n+1} = s^{n+1} + K(\Delta\boldsymbol{\epsilon} : I)I \tag{29}$$

$$c^{n+1}\frac{\partial\boldsymbol{\sigma}^{n+1}}{\partial\Delta\boldsymbol{\epsilon}} = KI \otimes I + 2G\beta\left(II - \frac{1}{3}I \otimes I\right) - 2G\bar{\gamma}\bar{n} \otimes \bar{n} \tag{21}$$

where

$$\beta = \sqrt{\frac{2}{3}}\frac{A(c^{n+1}) - a\sqrt{\dfrac{3}{2}}P\Delta c}{\left|\boldsymbol{\xi}^{trial}\right|}$$

$$\bar{\gamma} = \frac{1}{1 + \dfrac{\dfrac{1}{a}\sqrt{\dfrac{3}{2}}\left(\dfrac{\partial A}{\partial c}\right)^{n+1} - \dfrac{3}{2}P}{3G}} - (1 - \beta)$$

$\varphi = 0$

Figure 3. PT-surface with isotropic hardening and kinematic softening.

Box 2. Finite element solution algorithm.

1. Initialization at t_n. Data structure: variables at quadrature points $\{c, \epsilon_t, \sigma\}^n$. Initial conditions for the increment of the displacement vector at nodal points $\{u\}^{n+1} = 0$. Current values of boundary conditions.

2. Let $\{u\}_k^{n+1}$ be solution at k-th iteration.

    2.1 Compute $\{\Delta\epsilon\}_k^{n+1} = \{(\nabla u)_s\}_k^{n+1}$ at quadrature points.

    2.2 Compute $\{\sigma, c, \epsilon_t\}_k^{n+1}$ at quadrature points according to the radial return algorithm (Box 1) and substep integration procedure [Idesman et al. (1999)].

    2.3 Compute the consistent tangents at quadrature points [Equation (21)].

    2.4 Compute residuals of the equilibrium equation $\{\Psi\}_k^{n+1}$

    $$\{\Psi\}_k^{n+1} := \{f\}^{n+1} - \int_V ([B]^t)\{\sigma\}_k^{n+1} dV$$

    ($\{f\}^{n+1}$ is the standard FE load vector, $[B]$ is the standard B-matrix), IF $\left\|\{\Psi\}_k^{n+1}\right\| < $ TOL GO TO 4 (TOL is a prescribed small number).

3. Solve system

    $$[K]\{\Delta u\}_k^{n+1} = \gamma\{\Psi\}_k^{n+1}$$

    where $[K] = \int_V ([B]^t)[c^{n+1}][B]dV$ is the consistent tangent stiffness matrix (for the first iteration $[K] = \int_V ([B]^t)[E][B]dV$ is the elastic stiffness matrix), γ is a parameter which is defined from numerical experiments, $\gamma \in [0,1]$. For the simplest case $\gamma = 1$. Update $\{u\}_{k+1}^{n+1} = \{u\}_k^{n+1} + \{\Delta u\}_k^{n+1}$. Set $k = k + 1$ and GO TO 2.

4. Update data structure

    $$\{c, \epsilon_t, \sigma\}^{n+1} = \{c, \epsilon_t, \sigma\}_k^{n+1}$$

and II is the fourth-order symmetric unit tensor with components $(1/2)(\delta_{ik}\delta_{jl} + \delta_{il}\delta_{jk})$; δ_{ik} is the Kronecker delta. A finite element algorithm for solving the boundary value problem is described in Box 2. It includes the iterative computation of the unknowns $\{c, \epsilon_t, \sigma\}^{n+1}$ at time $n + 1$ using the calculated values of these parameters at time n. According to the algorithm, it is not necessary to calculate the total displacements.

NUMERICAL MODELING

The model problems considered in this section are motivated by our collaboration with an experimental group comprised of Professor E. Hornbogen and Mr. J. Spielfeld of Ruhr-University of Bochum. The results presented below are used for the initial design and will be compared with future experiments.

Tube of SMA under Internal Pressure

Consider the loading of a tube from SMA (CuZnAl alloy) by internal pressure at ambient temperature, Figure 4. The solution of this simple axisymmetric problem can be used for verification of the SMA model for the 2-D case by comparison with experiments. The following elastic properties of the alloy were used in calculations [Levitas et al. (1998)]: Young's modulus $E = 0.58 \cdot 10^5$ MPa, Poisson ratio $\mu = 0.33$. The thermomechanical material parameters for SMA are determined by using the simple tension experiments by E. Hornbogen and J. Spielfeld according to the technique presented in the paper by Levitas et al. (1998) and given in Table 2.

The boundary conditions and the finite element mesh with quadratic triangular elements are shown in Figure 4, where u_n and u_τ are the normal and tangential displacements, σ_n and τ_n are the normal and shear stresses. The behavior of the tube was studied at different values of internal pressure $p = 0 - 50$ MPa. The results of calculations are analyzed and followed. Until $p = 30$ MPa, the tube is deformed elastically without transformation, see Figure 5(a). Then with increase of p, martensitic PT occurs and is extended from the internal radius of the tube to the external one. Distribution of the volume fraction of martensite along the radius for the section AB is presented in Figure 6. It can be seen that at $p = 35$ MPa, transformation is extended until the middle of the section, Figure 6(a). At $p = 45$ MPa, transformation occurs in the whole section, Figure 6(c). The maximum value of the volume fraction of martensite ($\approx 71\%$) is reached at the internal radius of the tube at $p = 50$ MPa, Figure 6(d). The inhomogeneous distribution of parameters along vertical axes in the upper part of the tube is caused by free surface AB, Figures 5(a), 7. Distribution of the radial displacement along the radius at the surface AB for different internal pressure p is presented in Figure 8 and can be easily measured in experiments.

Tube Assembly

Considered here is the modeling of one type of tube assembly with the help of an additional short tube from SMA [Hornbogen (1991)]. The idea is as follows: at first we deform a tube II from SMA (initially in a pure austenitic state) by applying the internal pressure at low temperature, transforming it completely into martensitic state. Due to residual transformation strains the internal diameter of the SMA tube II after unloading (Figure 9) becomes bigger and we can freely insert into it two tubes I, which should be connected, (in Figure 9, only one tube I is shown, as the second one is symmetrically located with respect to axes X_1). After heating

Table 2. Material parameters.

$a = 0.0245$	$\Delta\psi_0 = -13.3$ MPa	$\Delta s_0 = -0.05$ MPa/K
$P = 544$ MPa	$b = 0.038$ MPa	$d = 1.3$ MPa

(a)   (b)

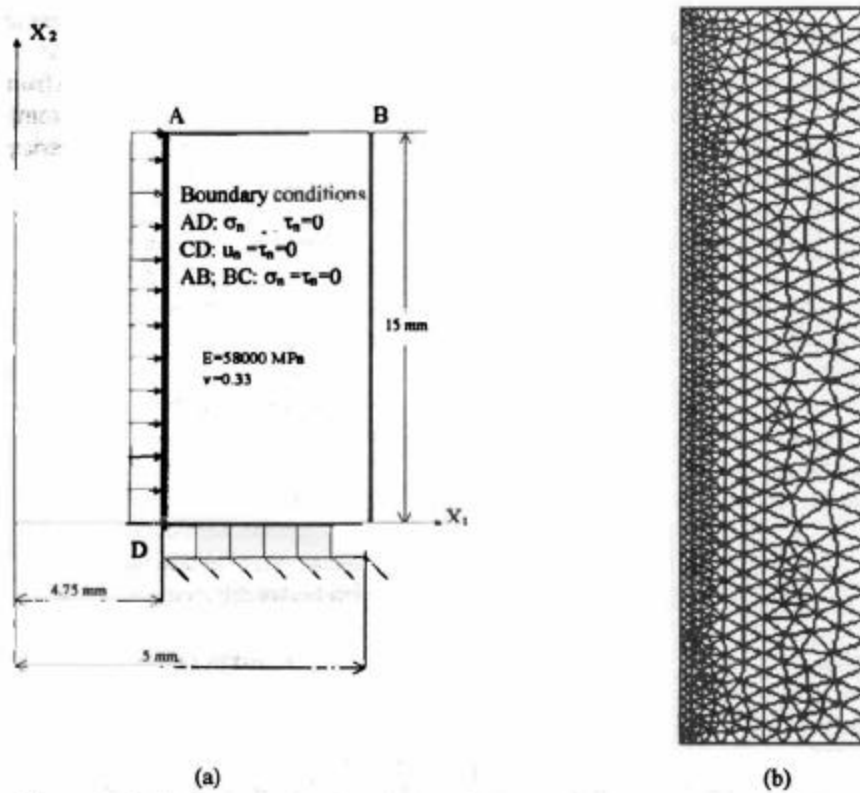**Figure 4.** A half of cross section of a tube from SMA (a) and FE (b). X_1 is the horizontal axis of symmetry, X_2 is the axis of rotation.

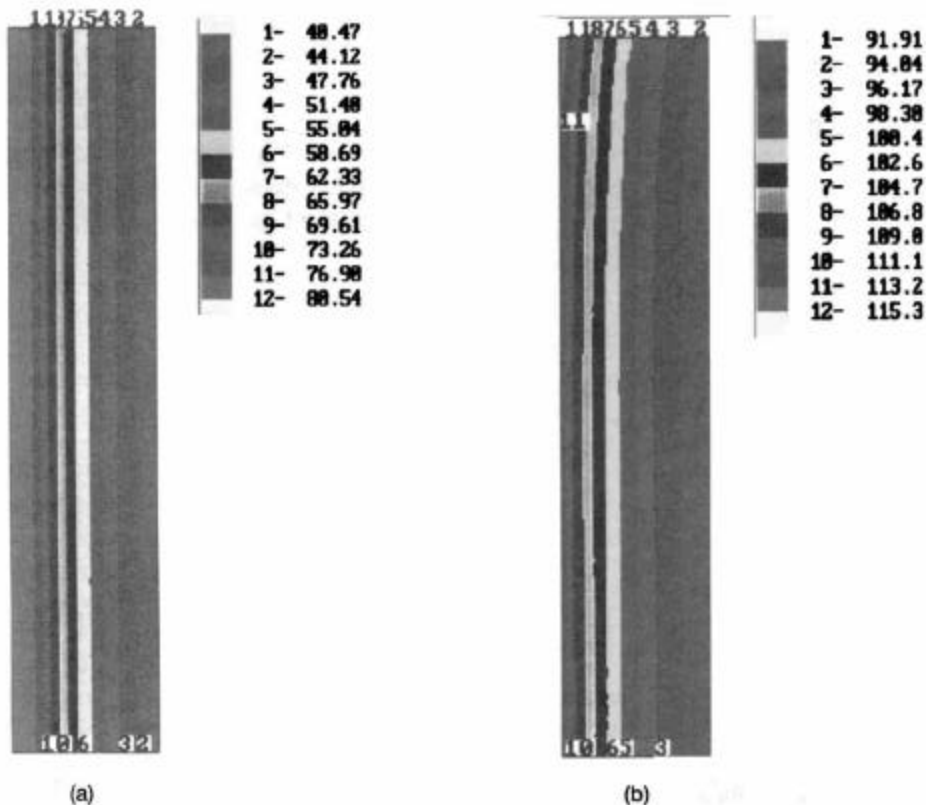|	
1–	40.47
2–	44.12
3–	47.76
4–	51.40
5–	55.04
6–	58.69
7–	62.33
8–	65.97
9–	69.61
10–	73.26
11–	76.90
12–	80.54

1–	91.91
2–	94.04
3–	96.17
4–	98.30
5–	100.4
6–	102.6
7–	104.7
8–	106.8
9–	109.0
10–	111.1
11–	113.2
12–	115.3

(a)   (b)

Figure 5. Distribution of the equivalent stresses in the sample at $p = 30$ MPa (a) and at $p = 50$ MPa (b).
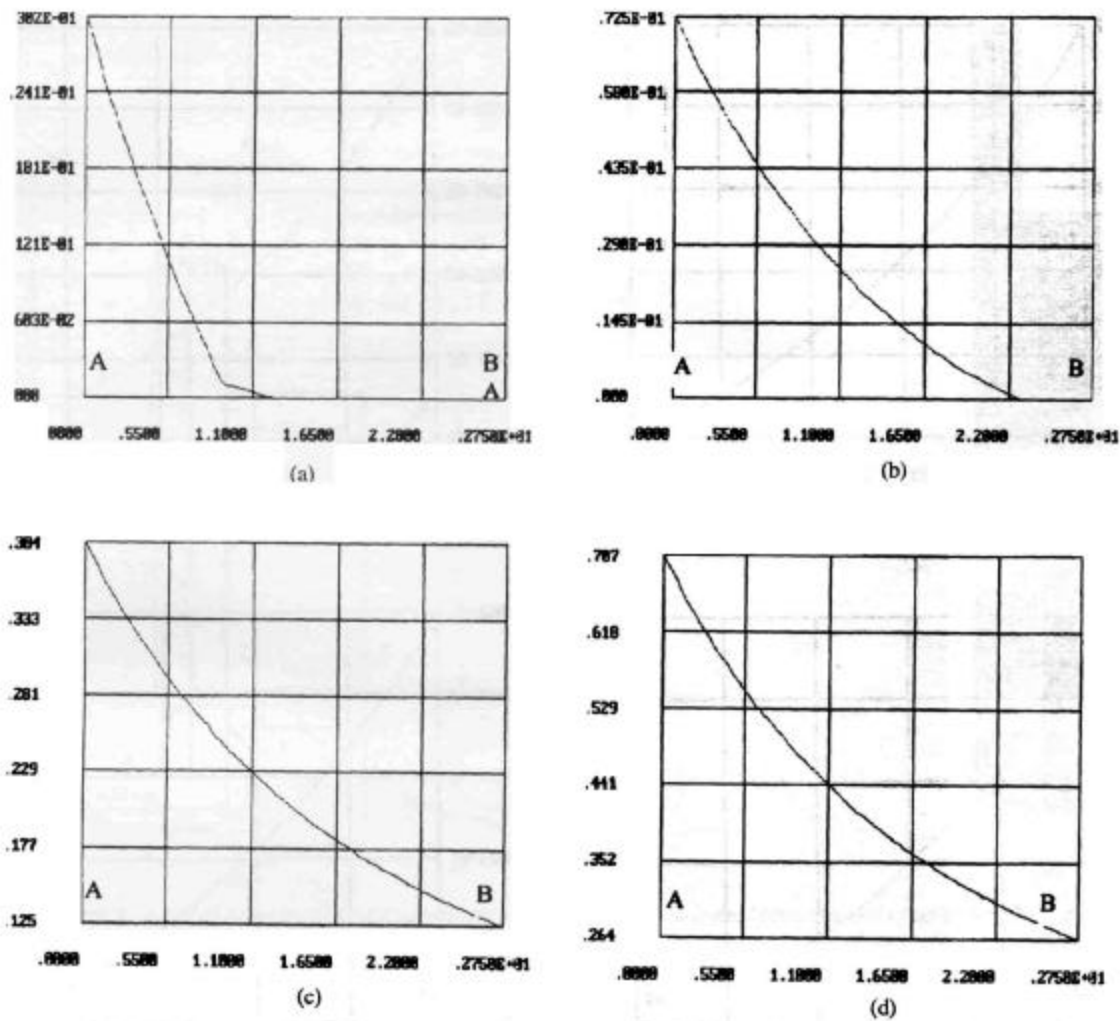
Figure 6. Distribution of the volume fraction of martensite along the radius AB: (a) at p = 35 MPa; (b) at p = 40 MPa; (c) at p = 45 MPa; (d) at p = 50 MPa.
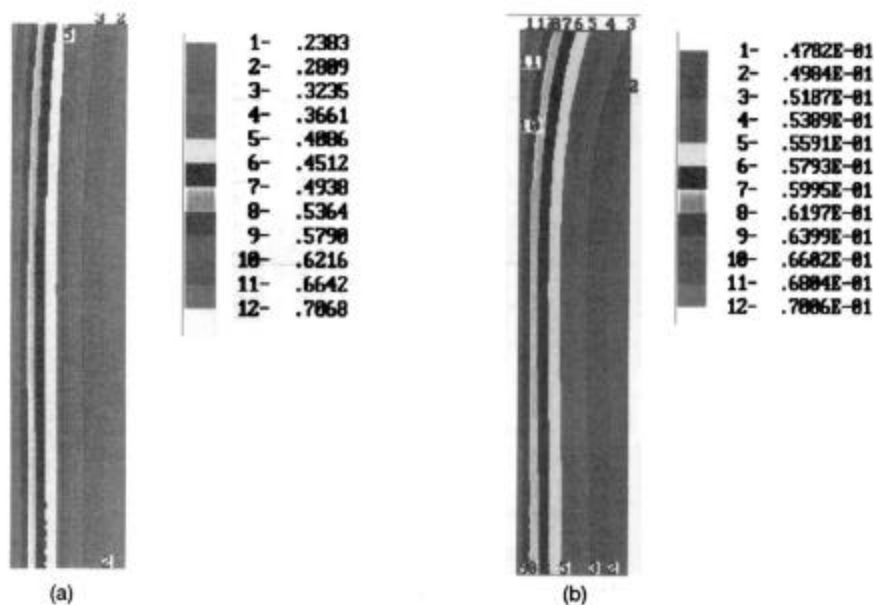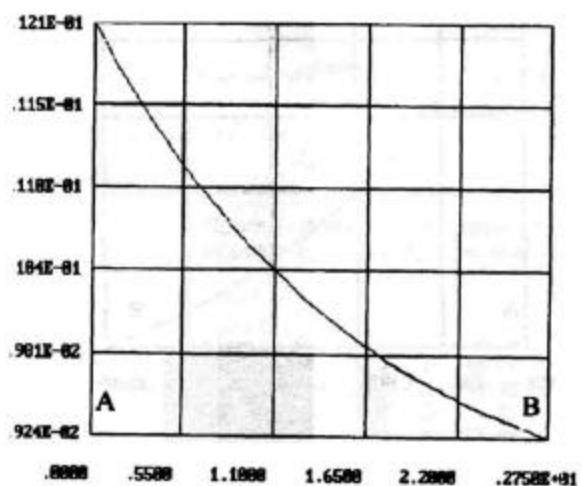

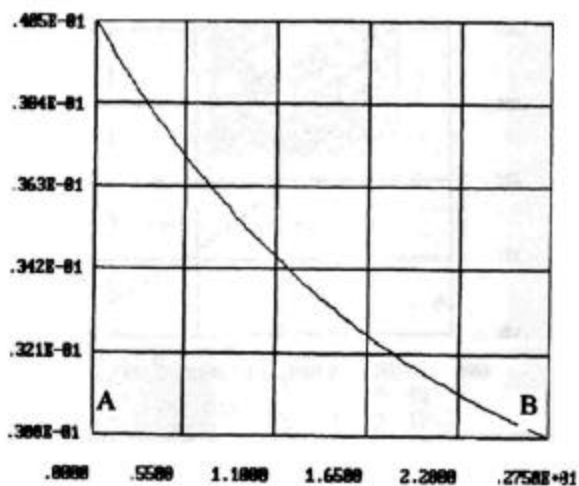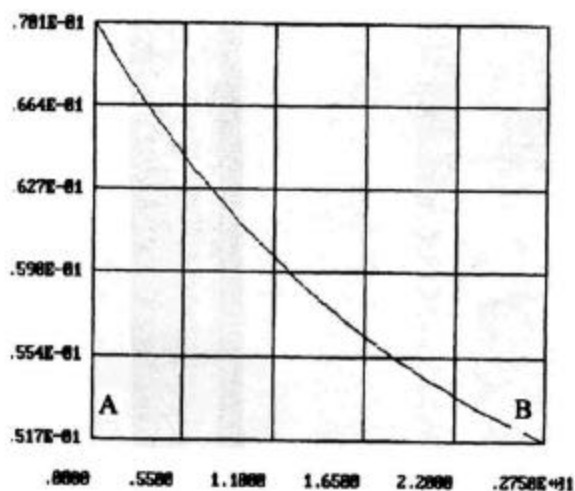**Figure 7.** Distribution of the volume fraction of martensite (a) and the radial displacement (b) in the sample at p = 50 MPa.
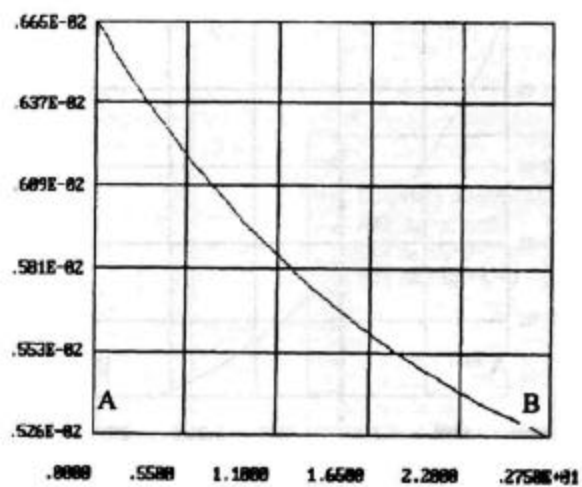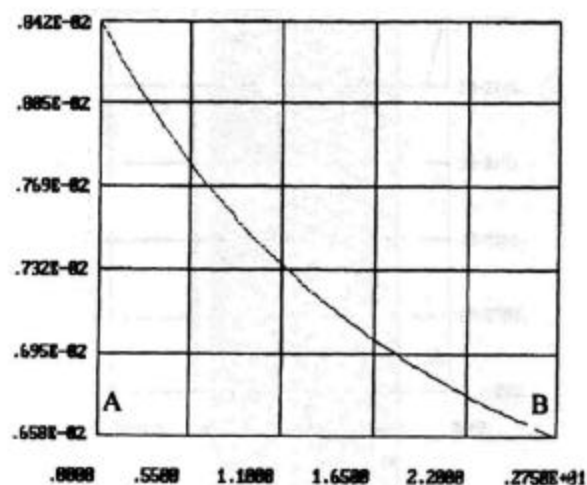
Figure 8. Distribution of radial displacements along the radius AB (c–e): (a) at p = 30 MPa; (b) at p = 35 MPa; (c) at p = 40 MPa; (d) at p = 45 MPa; (e) at p = 50 MPa.

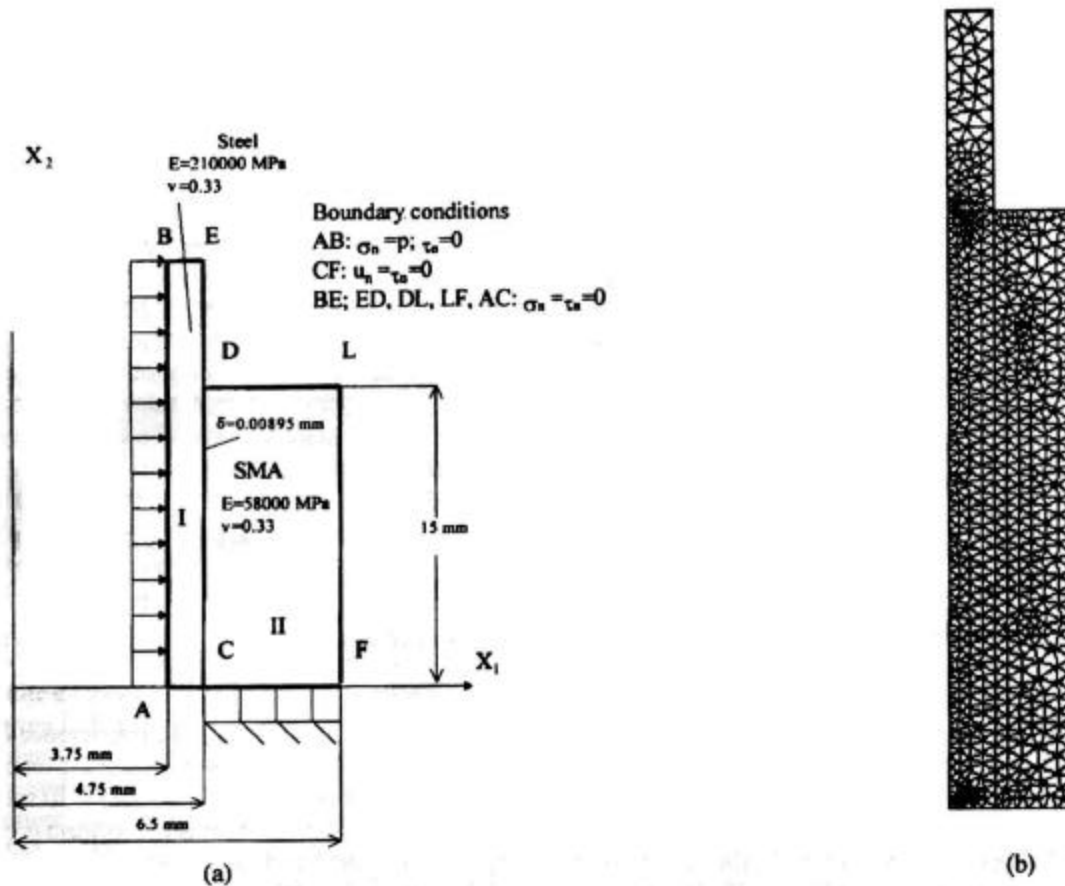**Figure 9.** A half of cross section of a sample (a) and FE mesh (b). X_1 is the horizontal axis of symmetry, X_2 is the axis of rotation.
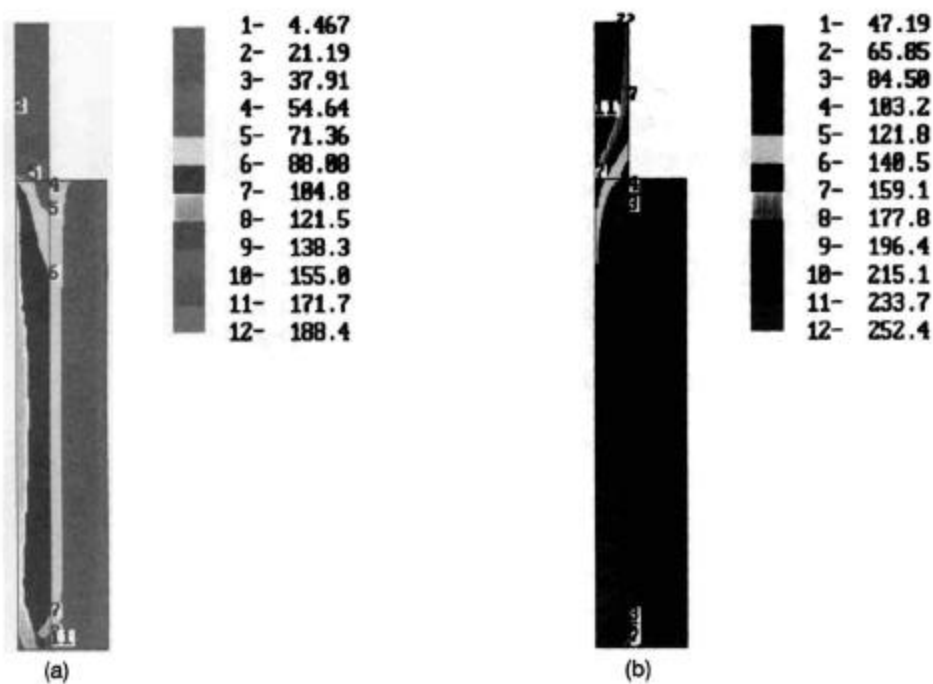

Figure 10. Distribution of the equivalent stress in the sample after assembly (a) and after loading at p = 50 MPa (b).
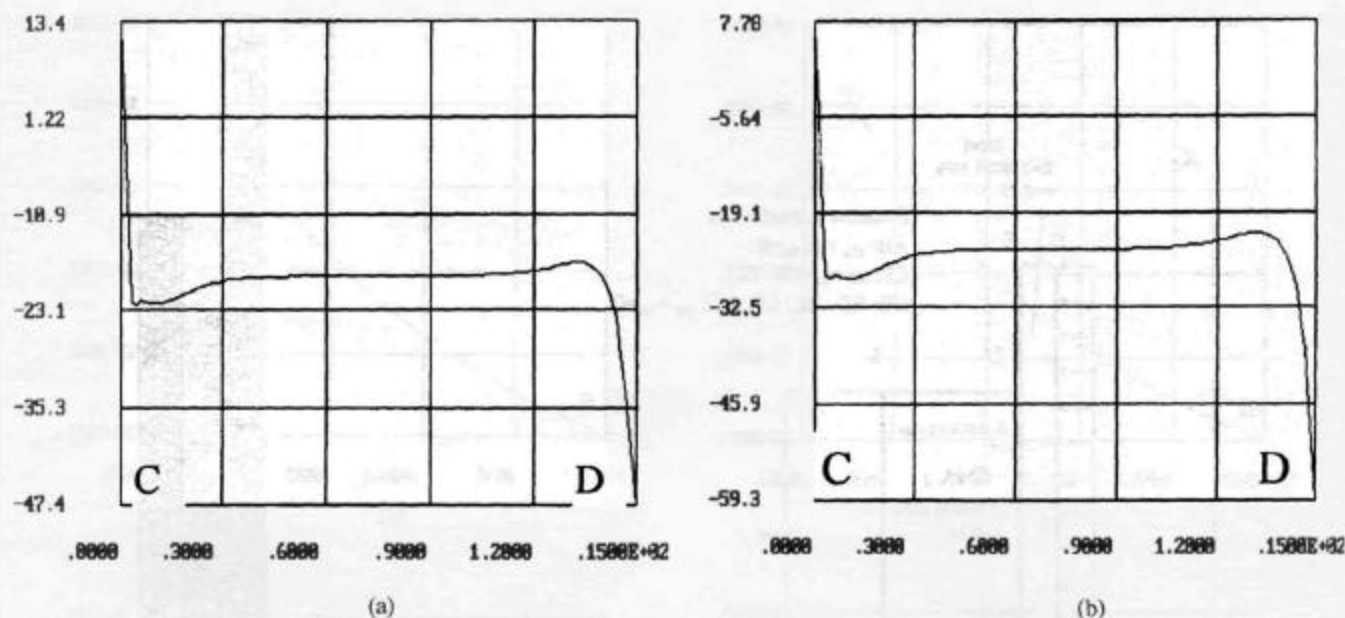
Figure 11. *Distribution of the radial stresses along surface CD in the tube from SMA after assembly (a) and at loading [p = 50 MPa (b)].*

to ambient temperature, reverse phase transition occurs in the whole SMA tube *II*, and it returns to its initial geometry. It causes compressive radial stresses at the interface between the tubes *I* and *II*. The higher these compressive radial stresses are, the firmer the connection is. As after assembly at ambient temperature, the SMA tube *II* should be in austenitic state (in order to reach the highest compressive radial stresses at the interface), we can model a stage of assembly as

a purely elastic problem with the interference δ at the interface which is equal to the difference of the internal radius of tube *II* and the external radius of tubes *I*. To solve this problem, we use the technique for elastic contact problems developed in the paper by Idesman and Levitas (1995). The value of the interference δ is chosen from the condition that after assembly the equivalent stresses $\sigma_i = \sqrt{3/2}\,|s|$ in the SMA tube do not exceed the pseudoyield stress $A\ (c = 0,\ \theta) = 80$
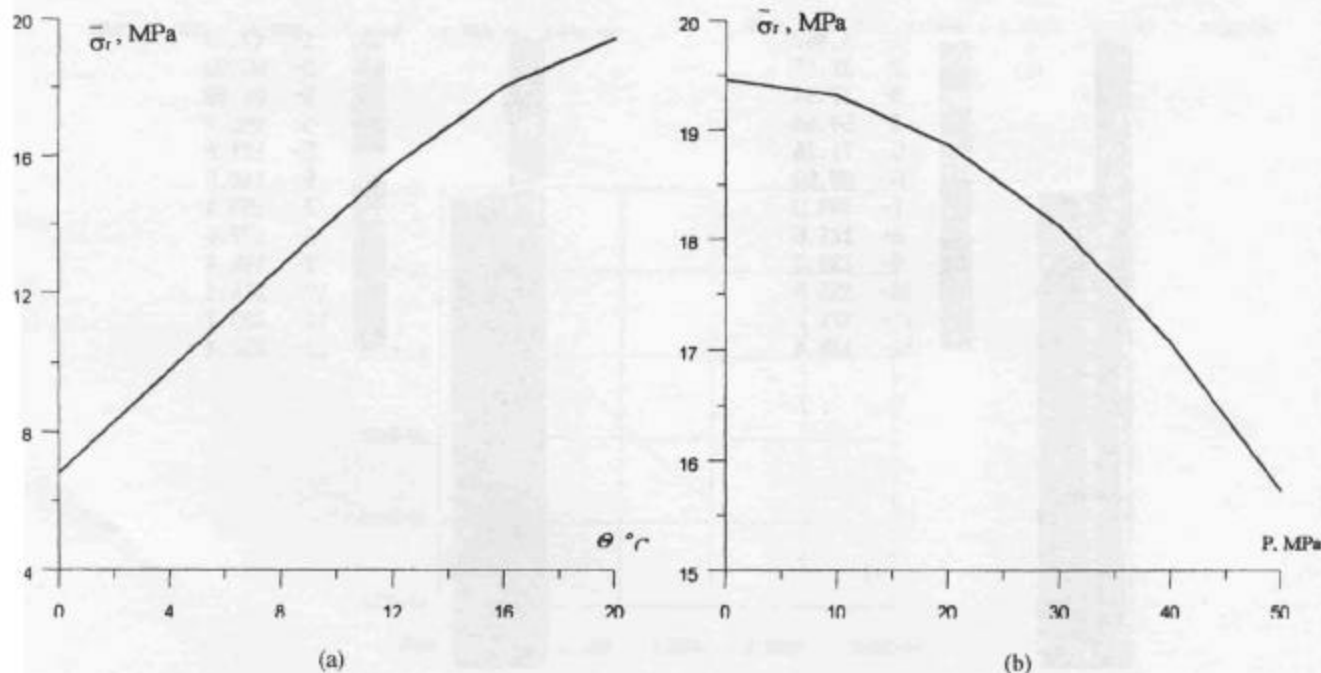

Figure 12. *(a) Relationship between the radial stresses $\bar{\sigma}_r$, averaged over surface CD, and temperature after cooling without loading. (b) Residual radial stresses $\bar{\sigma}_r$ (after unloading), averaged over surface CD, after loading at different values of internal pressure p and total unloading.*

MPa at ambient temperature. For simplicity, we have assumed a cohesion condition at interface (see also remark below).

After assembly, the following possible work stages are modelled: (a) loading of the assembly by internal pressure with subsequent unloading at ambient temperature; (b) cooling of the assembly without loading (for example, due to a variation of external temperature).

For both problems, stress-induced martensitic PT was studied based on the model presented in Table 1, i.e., reorientation of martensitic variants, reverse PT, as well as direct PT when an amplitude of transformation strain in the nucleus does not reach its maximum possible value [as, e.g., for temperature-induced PT, see Levitas and Stein (1997)] were not included. Stress-strain state in the tubes after assembly was used as initial conditions for the solutions of the problems (a) and (b).

Due to symmetry with respect to horizontal axes, a half of a cross section is considered, Figure 9. The properties of the tube of SMA are the same as in the previous problem. Elastic properties of steel tubes to be connected, boundary conditions and finite element mesh with quadratic triangular elements are given in Figure 9.

The distributions of the equivalent stresses in the tubes after assembly and at $p = 50$ MPa are presented in Figure 10. The distribution of the radial stresses at the interface *CD* is practically homogeneous except for the corner points *C* and *D* where stress concentration takes place, see Figure 11. The stage of loading by internal pressure p, accompanied by martensitic PT, and subsequent pure elastic unloading lead to a decrease in the residual radial stress averaged over interface
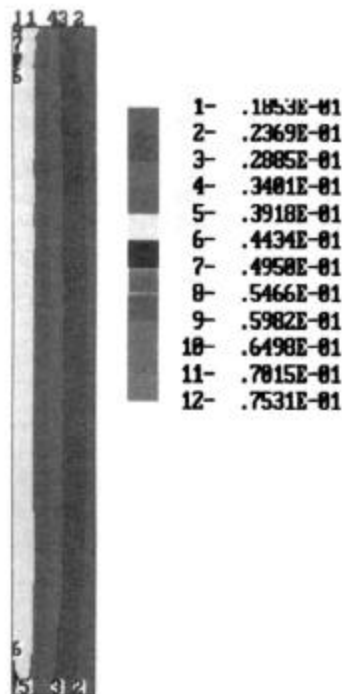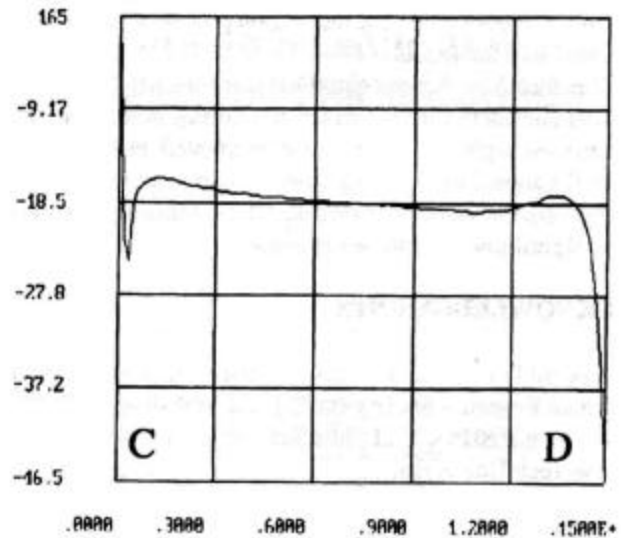

Figure 14. *Distribution of radial stresses along surface CD in the tube from SMA at pulling out of the steel tubes (contact problem).*

CD, see Figure 12(b). The rate of the decrease is higher at large values of p, see Figure 12(b). However, the amplitude of this decrease is relatively small, even at high p. More dangerous is the stage of cooling of the assembly without loading, because the pseudoyield stress reduces significantly with the temperature decrease for this material [Levitas et al. (1998)]. Due to stress-induced martensitic transformation caused by internal stresses in the system, the radial stress averaged over interface *CD* is much smaller (one half) at 4°C than at ambient temperature 20°C, see Figure 12(a). The distribution of the volume fracture of martensite in the SMA tube at 4°C is shown in Figure 13.

The influence of interfacial friction on the radial stress averaged over interface *CD* is not very essential. The solution of the contact problem simulating pulling out the steel tube *I* from the SMA tube *II* after assembly at ambient temperature [a normal displacement was applied at surface *BE*, and the friction coefficient at the interface *CD* was assumed to be 0.2, Figure 9(a)] has shown the decrease of the radial stress averaged over interface *CD* is not more than 7.5% (the distribution of the radial stress along interface *CD* for this case is given in Figure 14).

CONCLUDING REMARKS

The micromechanical derivation of the macroscopic associated transformation flow rule is carried out for the case of linear elasticity with equal elastic properties of phases and small strains. The method used is based on direct calculation of the transformation work which is very difficult to do without the above assumptions. For more complicated situations (finite strains, nonlinear elasticity, plastic deformations) other methods have to be developed. They can be based on internal variable theory [Rice (1971), Nemat-Nasser (1975)] or rate form of constitutive equations with PT [Levitas (1992,

1-	.1853E-01
2-	.2369E-01
3-	.2885E-01
4-	.3401E-01
5-	.3918E-01
6-	.4434E-01
7-	.4950E-01
8-	.5466E-01
9-	.5982E-01
10-	.6498E-01
11-	.7015E-01
12-	.7531E-01

Figure 13. *Distribution of the volume fraction of martensite in the SMA tube at $\theta = 4$°C.*

1996)]. For both cases, the nucleation process must be incorporated into the model.

It is fortunate that the simplest micromechanically-based model considered in this paper, the known numerical algorithm used in plasticity theory can be adapted. For more complex situations, when self-accommodation and reorientation of martensitic variants or reverse PT are taken into account, new algorithms have to be developed.

ACKNOWLEDGMENTS

REFERENCES

Idesman, A. V. and Levitas, V. I. 1995. "Finite element procedure for solving contact thermoplastic problems at large strain, normal and high pressures," *Comp. Meth. in Appl. Mech. and Eng.*, 126:39–66.

Idesman, A. V., Levitas V. I. and Stein, E. 1999. "Elastoplastic materials with martensitic phase transition and twinning at finite strains: numerical solution with the finite element method," *Comp. Meth. in Appl. Mech. and Eng.*, 173:71–98.

Havner, K. S. 1971. "A discrete model for the prediction of subsequent yield surfaces in polycrystalline plasticity," *Int. J. Solids and Structures*, 7:719–730.

Hill, R. 1967. "The essential structure of constitutive laws for metal composites and polycrystals," *J. Mech. Phys. Solids*, 15(2):79–95.

Hornbogen, E. 1991. *Legierungen mit Formgedächtnis*. Rheinisch-Westfälische Akademie der Wissenschaften (Vorträge, 338), Westdeutcher Verlag.

Lagoudas, D. C., Bo, Z. and Qidwai, M. A. 1996. "A unified thermodynamic constitutive model for SMA and finite element analysis of active metal matrix composites," *Composite Materials and Structures*, 3:153–179.

Leblond, J. B., Devaux, J. and Devaux, J. C. 1989. "Mathematical modeling of transformation plasticity in steels I: Case of ideal-plastic phases," *Int. J. Plasticity*, 5:551–572.

Leblond, J. B. 1989. "Mathematical modeling of transformation plasticity in steels II: Coupling with strain hardening phenomena," *Int. J. Plasticity*, 5:573–591.

Levitas, V. I. 1992. *Thermomechanics of Phase Transformations and Inelastic Deformations in Microinhomogeneous Materials*, Naukova Dumka, Kiev.

Levitas, V. I. 1995. "The postulate of realizability: formulation and applica-

tions to post-bifurcation behaviour and phase transitions in elastoplastic materials, Part 1 and Part 2," *Int. J. Eng. Sci.*, 33(7):921–971.

Levitas, V. I. 1996. "Some relations for finite inelastic deformation of microheterogeneous materials with moving discontinuity surfaces," in *IUTAM Symposium on Micromechanics of Plasticity and Damage of Multiphase Materials, Proceedings of IUTAM Symposium, Paris*, (eds. A. Pineau and A. Zaoui), 313–320.

Levitas, V. I. and Stein, E. 1997. "Simple micromechanical model of thermoelastic martensitic transformations," *Mech. Res. Commun.*, 24(3):309–318.

Levitas, V. I. 1998. "Thermomechanical theory of martensitic phase transformations in inelastic materials," *Int. J. Solids and Structures*, 35(9–10):889–940.

Levitas, V. I., Idesman, A. V., Stein, E., Spielfeld, J. and Hornbogen, E., 1998. "A simple micromechanical model for pseudoelastic behavior of CuZnAl alloy," *J. Intelligent Material Systems and Structures*, 9:324–334.

Mandel, J. 1966. "Contribution theoretique a l'etude de l'ecrouissage et des lois de l'ecoulement plastique" in *Proceedings Eleventh International Congress of Applied Mechanics, Berlin 1964*, Springer-Verlag Berlin, 502–509.

Nemat-Nasser, S. 1975. "On nonequilibrium thermodynamics of viscoelasticity: inelastic potentials and normality conditions" in *Mechanics of visco-elastic media and bodies*, (ed. J. Hilt), Springer-Verlag, Berlin, 375–391.

Patoor, E., Eberhardt, A. and Berveiller, M. 1996. "Micromechanical modelling of superelasticity in shape memory alloys," *Journal de Physique IV*, Colloque C1, 6:277–292.

Pradeilles-Duval, R.-M. and Stolz, C. 1993. "General relationships for heterogeneous materials with moving discontinuities," *MECAMAT 93*, Eurolles, Paris, 140–151.

Rice, J. R. 1971. "Inelastic constitutive relations for solids: an internal variable theory and its application to metal plasticity," *J. Mech. Phys. Solids*, 19:433–455.

Rogueda, C., Lexcellent, C. and Bocher, L. 1996. "Experimental study of pseudoelastic behavior of a CuZnAl polycrystalline shape memory alloy under tension-torsion proportional and non-proportional loading tests," *Arch. Mech.*, 48(6):1025–1045.

Simo, J. C. and Taylor, R. T. 1985. "Consistent tangent operators for rate-independent elastoplasticity," *Comput. Methods Appl. Mech. Engrg.*, 48:101–118.

Simo, J. C. and Hughes, T. J. R. 1998. Computational inelasticity. Springer-Verlag New York, Inc.

Sun, Q. P. and Hwang, K. C. 1993. "Micromechanics modelling for the constitutive behavior of polycrystalline shape memory alloys, Part 1 and Part 2," *J. Mech. Phys. Solids*, 41(1):1–33.

Tanaka, K. and Nishimura, F. 1998. "Thermomechanical behavior of an Fe-based shape memory alloy: Transformation conditions and hysteresis," *Metals and Materials*, 4(3):554–561.

Wayman, C. M. 1964. *Introduction to the Crystallography of Martensitic Transformation*, N.Y., Macmillan.